Talbot-defocus multiscan tomography to study the lacuno-canalicular network in mouse bone

Osteocytes may possibly be direct involved in bone remodeling [1]. However, definite evidence has not yet been reported. The cells involved in bone remodeling consist of osteocytes for detecting mechanical stress, osteoblasts for bone formation, and osteoclasts for bone resorption. Osteocytes extend their dendrites inside the canaliculi, which run in every direction, with a diameter of approximately 0.25 μm. A dendrite of one osteocyte comes into contact with a dendrite of another osteocyte through the gap junction. The canaliculi are also opened for bone marrow, vessels, and bone surfaces. Inside the bone, three dimensionally, the osteocytes are separeted from each other by a few tens of micrometers. Osteoblasts produce the collagen fiber, osteoid, at the surface of the bone. In the resting stage, osteoblasts degenerate into thin and flat forms distributed across the bone surface. Osteoclasts are over a few tens to hundred of micrometers in size and have a bone resorption ability. The osteoclasts resorb both collagen and mineral crystals at the bone surface, digest them and transport them to the opposite side and release the degraded products outside of the cell. When a fracture occurs, bone remodeling is initiated and the bone is repaired. Conventionally, the mechanism is believed to be as follows. Osteocytes detect the fracture using canaliculi. Through the osteocyte canalicular network, a signal is transmited to the osteoblasts on the surface of the bone.

When the osteoblast receives the signal, it induces the differentiation of osteoclasts. The induced osteoclasts initiate resorption of the bone and burrow into the damaged area. On the surface of the resorbed edge, the osteoblasts align. They simultaneously form lamellar bone of approximately ≥10 μm thickness. During bone formation, a part of the osteoblast is embedded in the lamellar structure. The mechanism behind this remains unclear. The embedded osteoblasts extend dendrites to osteocytes, which exist inside the bone, and also extend to the bone surface. The embedded osteoblasts differentiate into osteocytes. The lamellar bones are stacked layer by layer, and the fractured bone is replaced by new bone. However, a recent study has reported the possibility that osteocytes are directly involved in bone remodeling [2].

To clarify this possibility, the following technical requirements are needed: (1) extract canaliculi three dimensionally. (2) detect the change of mineralization based on mineral metabolism surrounding the canaliculi, and (3) obtain a view that covers the complete osteocyte canalicular network.

The conventional methods have limitations. In most analyses, the bone specimens are decalcified using acids, the field of view is narrow, and the sensitivity of mineralization is low. In this study, we overcame these difficulties by developing a Talbot-defocus multiscan method that consists of two imaging techniques based on X-ray microscope tomography with synchrotron radiation [3]. The method employing a Talbot interferometer enables highly sensitive observations via X-ray differential phase contrast [4]. With this technique, we can estimate the degree of bone matrix mineralization. Moreover, the method using defocus absorption contrast [5] allowed the visualization of the canalicular network and the entire cortical thickness from the endosteum to the periosteum. These two methods scan the same region of the specimen sequentially.

The Talbot-defocus multiscan X-ray microscope was constructed at the undulator beamline **BL20XU**. Imaging was performed using monochromatic 9-keV X-rays (Fig. 1(a)). An X-ray Fresnel zone plate (FZP) was used as an objective lens with a focal length of 261 mm. The sample was set 273 mm upstream of the FZP in the on-focus condition. Images were recorded using a CCD camera. The image detector was placed at the image plane 5.71 m downstream of the FZP. Therefore, the X-ray microscope magnification was 20.9 times,

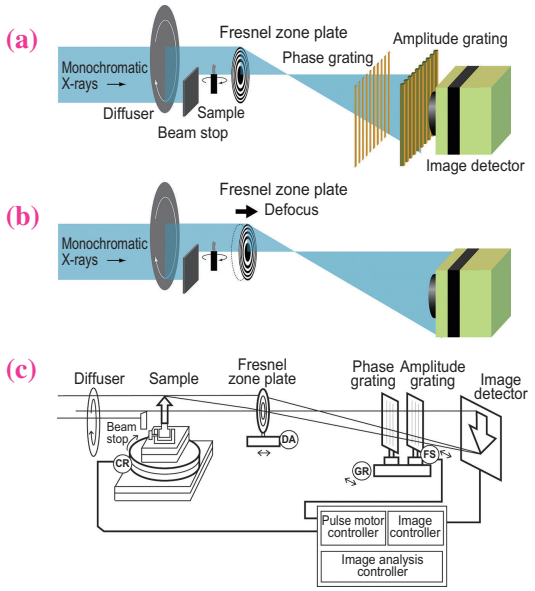

Fig. 1. Setup of multiscan X-ray microscope. **(a)** Differential phase-contrast mode in combination with a Talbot interferometer consisting of a phase grating and an amplitude grating. **(b)** Defocus absorption-contrast mode achieved by moving the Fresnel zone plate (thick arrow). **(c)** Block diagram of control system. FS, fringe scanning; GR, grating removal; DA, defocus arrangement; CR, CT scan rotation [3].

and the effective pixel size was 0.208 μm. The Talbot-defocus multiscan analysis was performed for each sample, as shown in Fig. 1(c). In the differential phase contrast method, CT scanning was performed with 500 projections over 180°. The total scan time was 6.5 h/sample.

In the defocus contrast method, the Talbot interferometer was removed from the optical axis. The FZP on the defocus stage was displaced 6 mm downstream along the optical axis in order to enhance the edge contrast of the object with Fresnel's diffraction effects. CT scan was performed with 1800 projections over 180°. The total scan time was 2.5 h/sample.

Tibias were isolated from euthanized 12–16-week-old female C57BL/6J mice (Clea, Tokyo, Japan). We applied the Talbot-defocus multiscan method to each cortical bone sample (Fig. 2).

Figure 3 shows a summary of the results. The Talbot phase tomogram revealed the degree of mineralization in the vicinity of osteocyte lacunae and canaliculi (Fig. 3(a)). The high mineralization zone observed near the periosteum and endosteum corresponds to the lamellar zone. The low mineralization zone located at the center of the cortical bone corresponds to the nonlamellar zone. The defocused setting image was reversed to demonstrate the osteocyte canalicular network (Fig. 3(b)). Canaliculi were enhanced as bright lines because of the defocus effect. In the lamellar zone, canaliculi ran parallel to each other, extending toward the bone surface (arrows). In contrast, at the middle of the cortical bone, the parallel arrangement of canaliculi was no longer apparent. Canaliculi corresponded precisely with each other in Figs. 3(a) and 3(b), as indicated by yellow arrows in Fig. 3(c). Thus, we detected the 3D structure of osteocyte canaliculi and the degree of mineralization in the vicinity of the osteocyte canalicular network in the merged image.

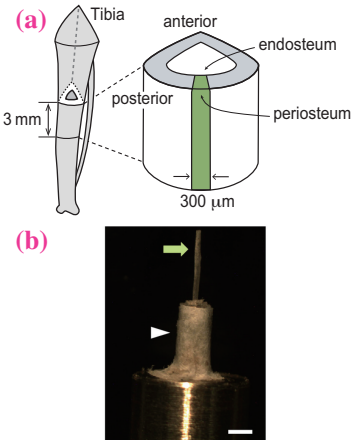

Fig. 2. Preparation of mouse bone sample. **(a)** Schematic presentation of tibia. The cortical bone sample used for imaging is represented in green. **(b)** The sample (green arrow)was attached to the holder using double-sided adhesive tape (arrowhead). Scale bar, 1 mm [3].

To detect the canaliculus, we employed a defocus absorption-contrast method to enhance the edge structure. Although the diameter of the canaliculus cannot be determined by this method, the location of abundant canaliculi was mapped as distinct lines in the tomogram. The Talbot phase tomogram revealed the distribution of mineralization, and combining the two tomograms allowed us to understand changes in mineralization in regions surrounding the osteocyte canalicular network. The spatial changes in mineralization suggest that osteocytes directly participate in mineral metabolism through the osteocyte canalicular network.

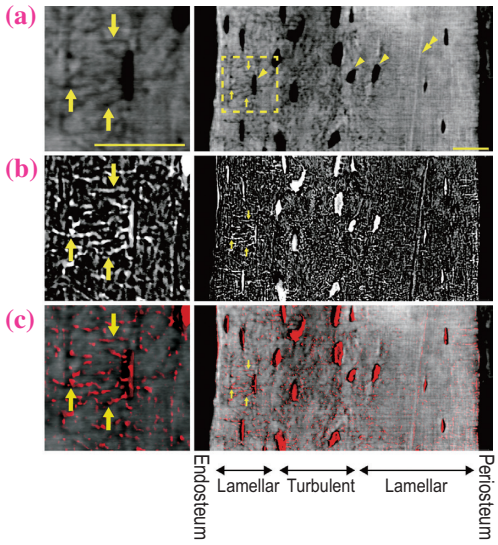

Fig. 3. Reconstructed tomograms. **(a)** Phase tomogram, in which gray scale indicates degree of mineralization (white, high; dark, low). Arrows, osteocyte canaliculi; Arrowheads, osteocyte lacunae; Double arrowhead, cement line. **(b)** Tomogram with defocus edge enhancement. The outer edges of the lacunae and canaliculi are enhanced. Note that black and white are reversed. **(c)** Combined image of (a) and (b). The defocus image is pseudocolored red. Scale bars, 25 μm. The dotted rectangle in (a-c) is magnified in the left image [3].

Nobuhito Nango[a,*], Koichi Matsuo[b] and Atsushi Momose[c]

[a] Ratoc System Engineering Co., Ltd.
[b] School of Medicine, Keio University
[c] Institute of Multidissciplinary Research for Materials, Advanced Tohoku University

*E-mail: nango@ratoc.co.jp

References

[1] L.F. Bonewald: J. Bone Miner. Res. **26** (2011) 229.
[2] T. Nakashima *et al.*: Nat. Med. **17** (2011)1231.
[3] *N. Nango, S. Kubota, A. Tkeuchi, Y. Suzuki, W. Yashiro, A. Momose and K. Matsuo: Biomed. Opt. Express* ***4*** *(2013) 917.*
[4] Y. Takeda *et al.*: Appl. Phys. Express **1** (2008) 117002.
[5] A. Snigirev *et al.*: Rev. Sci. Instrum. **66** (1995) 5486.